



	<b>Experiment title:</b> Control of sulfides dissolution by iron coating. Implications for passive treatment systems in natural conditions.	<b>Experiment number:</b> EC-632
<b>Beamline:</b> ID21	<b>Date of experiment:</b> from: 26/04/2010 to: 30/04/2010	<b>Date of report:</b> July 2012
<b>Shifts:</b> 9	<b>Local contact(s):</b> Marine Cotte	<i>Received at ESRF:</i>
<b>Names and affiliations of applicants</b> (* indicates experimentalists): <b>Maria P. Asta<sup>1*</sup>, Rafael Pérez-López<sup>2*</sup>, Gabriela Román-Ross<sup>3*</sup></b> Present affiliations: <sup>1</sup> School of Natural Sciences, University of California, Merced, 5200 North Lake Road, Merced, CA 95343, USA <sup>2</sup> Department of Geology, University of Huelva, Campus 'El Carmen', 21071, Huelva, Spain <sup>3</sup> Amphos 21, Passeig de Garcia i Faria, 49-51, 1-1, Barcelona, 08019, Spain		

## Report:

### **Aims of the experiment and scientific background**

Oxidation of pyrite and other minor sulphides is the major contributor of hydrogen ions in mine waters. This process, called Acid Mine Drainage (AMD) or Acid Rock Drainage (ARD), not only creates acidity but it also releases toxic metals, metalloids and sulphate into waters giving rise to a major environmental issue (Nordstrom & Alpers, 1999).

To minimize the oxidation of sulphide phases present in mine tailings, different treatment methods are used. These methods involve the passivation of the acid-generating material, thus protecting the sulphide surface from water and oxygen. The most common active treatment method in tailings is to increase the pH with an alkaline reagent such as hydrated lime, precipitating a sludge composed of poorly crystallized Fe-Al oxyhydroxides/oxy-hydroxysulphates often with significant concentrations of heavy metals and metalloids (e.g. copper, zinc, arsenic). This process has several positive effects: (1) acidity is neutralized; (2) iron and other metals are removed from the solutions and (3) the precipitation of Fe-phases on sulphides prevents and protects the grains from further contact with oxygen or other oxidizing agents by blocking the transport of oxidants to the mineral surface. This last process includes passivation and coating of the sulphide in presence of different alkaline substances.

Many of the previous studies regarding this issue have confirmed the presence of coatings or precipitates on rock and tailing surfaces by using scanning electron microscopy (SEM), X-ray diffraction (XRD), and XPS. In addition, the decrease of iron levels in drainage was often cited as evidence of coating formation and/or

iron precipitation. Despite the valuable insights given by the techniques used in previous studies, they do not provide the capability to evaluate the compositional and mineralogical variation with micrometer spatial resolution. Therefore, in this experiment the precipitates formed during marcasite and arsenopyrite oxidation under neutral to basic conditions have been characterized by micro-X-ray absorption near edge structure ( $\mu$ XANES).

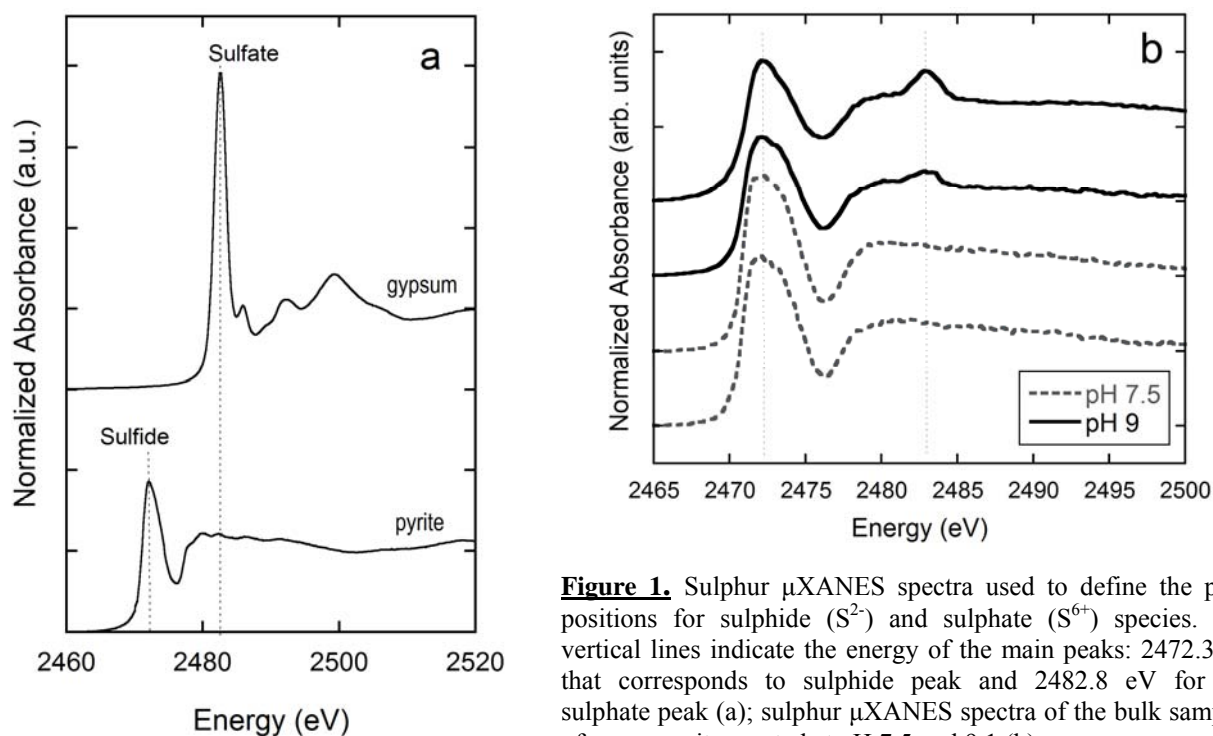
## Experimental methodology

Sulphur and iron  $\mu$ XANES spectra were acquired at S and Fe K-edges (2500 and 7200 keV, respectively) using a Si(111) monochromator crystal for S and a Si(220) crystal for Fe. All spectra were collected in X-ray fluorescence (XRF) mode with a single-element silicon drift diode (SDD) detector (Bruker AXS, Germany), unfocused beam and beam size  $0.21 \times 0.81 \mu\text{m}^2$  (ver. $\times$ hor.) for sulphur and  $0.31 \times 1.1 \mu\text{m}^2$  (ver. $\times$ hor.) for iron. For all Fe  $\mu$ XANES data, beam energy was calibrated on an Fe foil with the first edge inflection set to 7112 eV. For S XANES, the monochromator calibration was done, setting the peak value of a gypsum reference to 2482.8 eV. For both elements, in each studied spot, three scans were collected and averaged. Background subtraction and data normalization was performed using the Athena software program (Ravel and Newville, 2005). To map the distribution of oxidized and reduced states of sulphur, energy difference XRFmaps were performed at three different energies (2472.3, 2482.8 and 2500 eV), which correspond to maximum absorption in the edge region for different S species. In the case of Fe XRFmaps, they were obtained at 7200 eV.  $\mu$ XRF spectra were collected in each pixel of the 2D images and were treated with PyMCA software (Solé *et al.*, 2007) and then elemental maps were obtained through a batch treatment.

## Results

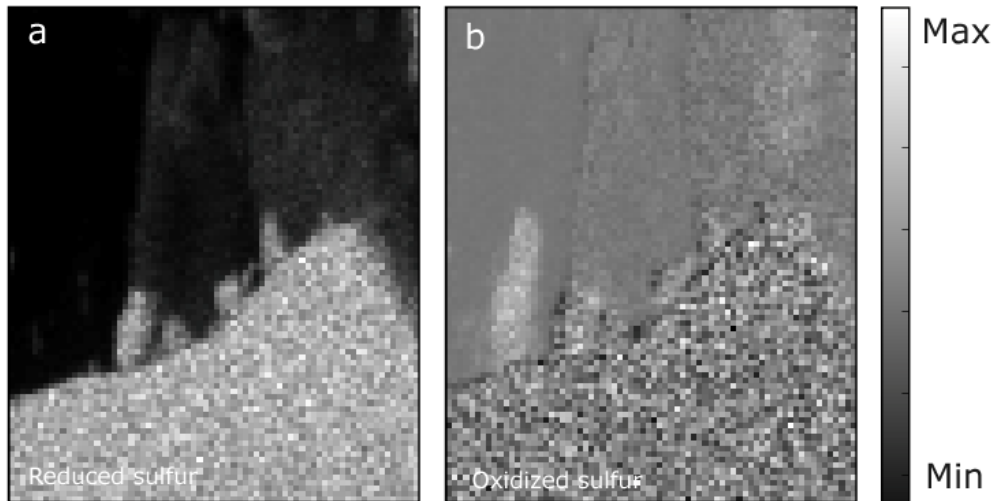
### S K-edge X-ray Absorption Near Edge Structure

Figure 1a shows the  $\mu$ XANES spectra of two reference minerals used to define the position and the features associated with  $\text{S}^{2-}$  and  $\text{S}^{6+}$  sulphur species. These spectra were taken from the ID21 sulphur XANES spectra database. Figure 1b shows the average of the normalized  $\mu$ XANES spectra at the S K-edge of the bulk samples of arsenopyrite reacted at pH 7.5 and 9. The spectra show, in all samples, the characteristic broad peak at 2472.1 eV observed in pyrite indicating the predominance of sulphide in the samples. In addition, the samples reacted at pH 9 show a small shoulder at 2482.5 eV that is consistent with minor amounts of sulphate in the sample. Therefore, the results indicate a variation in sulphur species with pH and an increase of the sulphate content as pH increased.



**Figure 1.** Sulphur  $\mu$ XANES spectra used to define the peak positions for sulphide ( $\text{S}^{2-}$ ) and sulphate ( $\text{S}^{6+}$ ) species. The vertical lines indicate the energy of the main peaks: 2472.3 eV that corresponds to sulphide peak and 2482.8 eV for the sulphate peak (a); sulphur  $\mu$ XANES spectra of the bulk samples of arsenopyrite reacted at pH 7.5 and 9.1 (b)

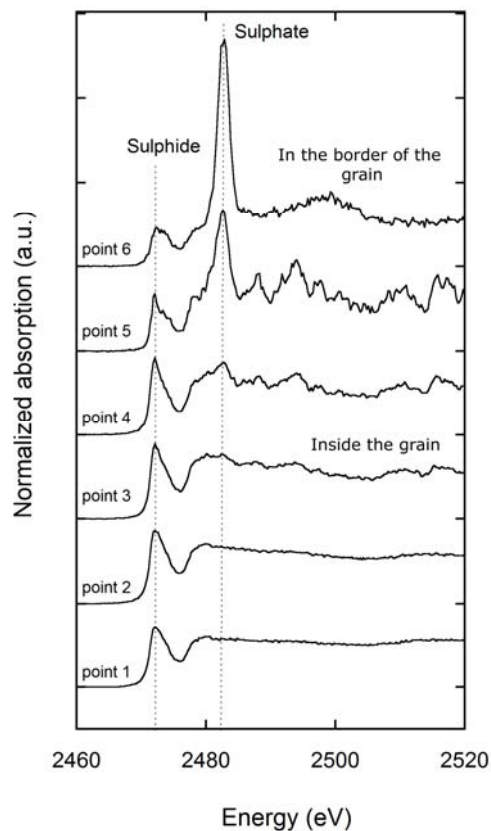
To map the distribution of oxidized and reduced states of sulphur in the sample a simple method was used (Cotte *et al.*, 2006). The results showed that sulphates are mainly located in the border of the grain (Figure 2). In addition,  $\mu$ XANES spectra of different points from an area inside a grain to the border of the grain were performed (Figure 3).



**Figure 2.** Normalized images of the distribution of the reduced (a) and oxidized sulphur (b) in the marcasite sample reacted at pH 12.4.

It is clearly observed a variation of the sulphur oxidation state in the sample, being the sulphates concentrated towards the border of the grain. Figure 3 show the XANES spectra obtained in different points of the sample. Points 1 to 3 were acquired inside the marcasite grain and they perfectly fit with the sulphide feature with a peak at 2472.1 eV and with little or no detectable sulphate. However, points 4, 5 and 6, acquired in the layer that covers the grain, showed a peak at 2482.5 eV corresponding to sulphates. The relative intensity of the sulphate peak is higher in the points 5 and 6 located out of the marcasite grain.

**Figure 3.** X-Ray absorption spectra at the S K-edge obtained in different points of the fluorescence maps.



## Fe K-edge X-ray absorption near edge structure

The spatial variation of the iron oxidation state of a selected sample of arsenopyrite reacted at pH 9 was studied by analyzing different spots of the sample (Figure 4a). The normalized  $\mu$ XANES spectra and corresponding first-derivative for different points along the sample and three reference compounds are shown in figure 4b. All the Fe  $\mu$ XANES spectra of the reacted sample are clearly different from the Fe oxides and more similar to the Fe sulphide model compound shown (pyrite). The normalized first derivative of iron  $\mu$ XANES of the reacted sample shows a peak inflection at pre-edge 7112.0-7112.3 eV, a primary peak inflection at 7118.3-7118.5 eV and a small peak at 7130 eV. These main derivative peaks correspond to those assigned to Fe in sulfides (see e.g., O'Day *et al.*, 2004). The presence of a small shoulder at higher energies could suggest the presence of an Fe oxide component which would increase toward the border of the grain (Fig. 4b, point 4). Linear combination fitting of the reacted samples XANES spectra was conducted over the Fe- XANES region. After considering different Fe-compounds (e.g. goethite, ferrihydrite, hematite) the results showed that magnetite could contribute to the spectra but in low percentages (Figure 4c, point 4).

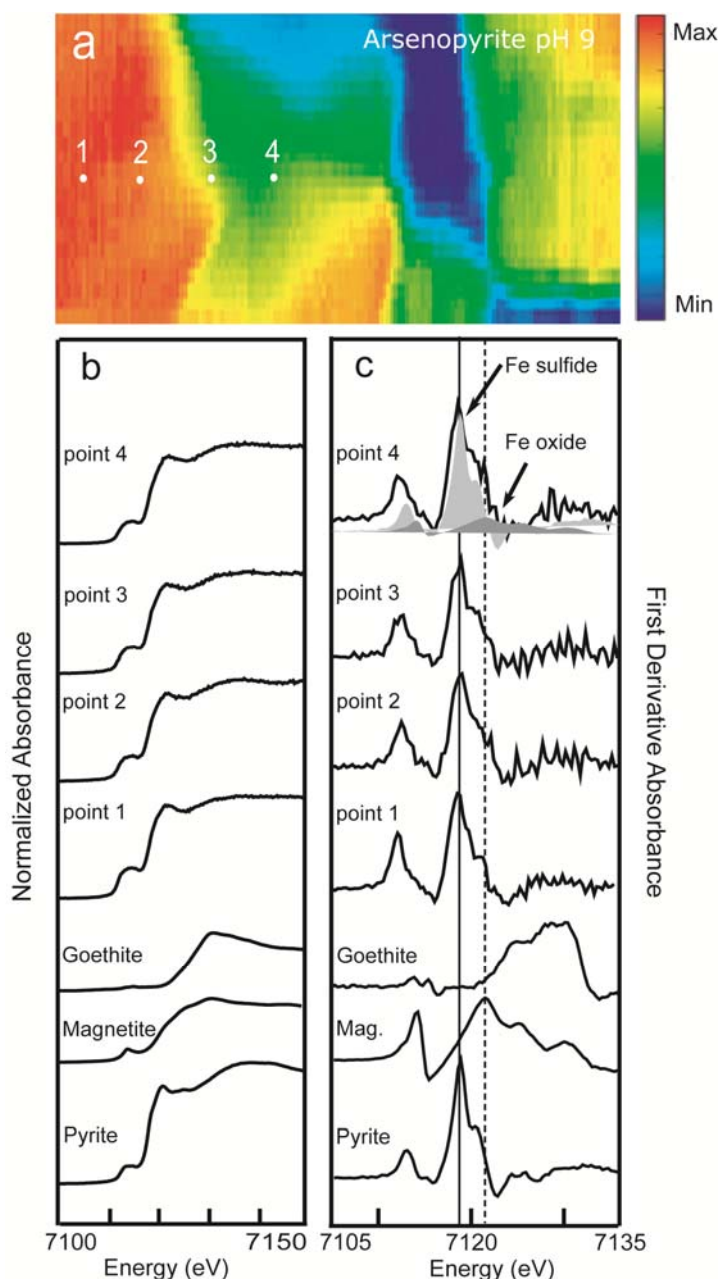


**Figure 4.** Iron fluorescence map of the arsenopyrite reacted at pH 9 obtained at 7200 eV (a); Iron K-edge  $\mu$ XANES (b) and corresponding first-derivative spectra compared to reference spectra (c). Shading in the first-derivative spectra of point 4 shows the fraction of iron associated mainly to a sulphide phase (pyrite) and a minor Fe oxide phase (magnetite) after performing linear combination fit with Athena.

In addition to the study of the normalized Fe  $\mu$ XANES spectra and corresponding first derivative, the pre-edge features in the Fe  $\mu$ XANES spectra have been analyzed. As previously reported, the comparison of the pre-edge features of model compounds and reacted samples may provide insight of the oxidation state of the samples (Wilke *et al.*, 2001, 2009; Berry *et al.*, 2003; Métrich *et al.*, 2006). The Fe-K pre-edge features were extracted from the normalized spectra by selecting the 7105-7120 eV region. A spline function was then used to extract the pre-edge feature defining a smooth curve through the absorption edge using the data several eV before and after the pre-edge feature as used in previous studies (Wilke *et al.*, 2001; Berry *et al.*, 2003). The pre-edge extracted from spectra of two model compounds (pyrite as representative of Fe<sup>2+</sup> and ferrihydrite of Fe<sup>3+</sup>) and the reacted sample (points showed in figure 4) are presented in Fig. 5.

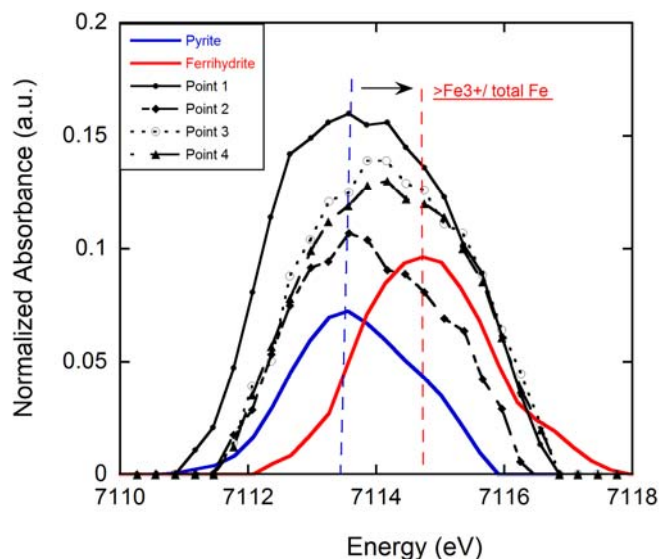


**Figure 5.** Normalized pre-edge spectra (Fe-K-edge) of model compounds and different  $\mu$ XANES spectra of the arsenopyrite sample reacted at pH 9.

As reported in previous studies (see e.g, Métrich *et al.*, 2006), the pre-edge shows a shift to higher energies with increasing the Fe<sup>3+</sup>/ $\Sigma$ Fe ratio. The results suggest that there is a mixture between Fe<sup>2+</sup> and Fe<sup>3+</sup> in the studied points but with predominance of Fe<sup>2+</sup>. In addition, the small shift observed when comparing the spectra from the center of the grain to the border may indicate an increase of the ferric iron in the border.

## Conclusions

The use of the synchrotron techniques has allowed us to characterize the composition of the coatings formed during the sulfides' dissolution under laboratory conditions. This information is of paramount importance since the long-term chemical stability of ARD-AMD treatment sludges resides on this coating effectiveness as metals retained could be released back into the environment if they are exposed to low pH water.

## Publications

The publication indicated below has been already submitted to European Journal of Mineralogy; its current status is: under review.

Asta, M.P., Pérez-López, R., Román-Ross, G., Illera, V., Cama, J., Cotte, M., Tucoulou, R. (2012). Analysis of the iron coatings formed during marcasite and arsenopyrite oxidation at neutral-basic conditions. *European Journal of Mineralogy*. Under review.

## References

- Berry, A.J., O'Neil, H. ST. C., Jayasuriya, K.D., Campbell, S.J., Foran, G.J. (2003): XANES calibrations for the oxidation state of iron in a silicate glass. *Am. Mineral.*, **88**, 963-977.
- Cotte, M., Susini, J., Métrich, N., Moscato, A., Gratzu, C., Bertagnini, A., Pagano, M. (2006): Blackening of Pompeian cinnabar paintings: X-ray microspectroscopy analysis. *Anal. Chem.*, **78**, 7484-7492.
- Métrich, N., Susini, J., Foy, E., Farges, F., Massare, D., Sylla, L., Lequien, S., Bonnin-Mosbah, M. (2006): Redox state of iron in peralkaline rhyolitic glass/melt: X-ray absorption micro-spectroscopy experiments at high temperature. *Chem. Geol.*, **231**, 350-362.
- Nordstrom, D.K. & Alpers, C.N. (1999): Negative pH, efflorescent mineralogy, and consequences for environmental restoration at the Iron Mountain Superfund site, California: *Proc. Natl. Acad. Sci. USA*, v. 96, p. 3455–3462.
- O'Day, P.A., Rivera Jr., N., Root, R., Carrol, S.A. (2004): X-ray absorption spectroscopic study of Fe reference compounds for the analysis of natural sediments. *Am. Mineral.*, **89**, 572-585.
- Ravel, B. & Newville, M. J. (2005): ATHENA, ARTEMIS, HEPHAESTUS: data analysis for X-ray absorption spectroscopy using IFEFFIT. *Synchrotron Radiat.*, **12**, 537-541.
- Solé, V.A., Papillon, E., Cotte, M., Walter, Ph., Susino, J. (2007): A multiplatform code for the analysis of energy-dispersive X-ray fluorescence spectra. *Spectrochim. Acta Part B*, **62**, 63-68.
- Wilke, M., Farges, F., Petit, P-E, Brown, G.E. Jr., Martin, F. (2001): Oxidation state and coordination of Fe in minerals: An Fe K-XANES spectroscopy study. *American Mineralogist*, **86**, 714-730.

